

Size Controlled Synthesis of γ -Fe₂O₃ Nanoparticles by Simple Chemical method and Study of Optical Properties

^[1] Ramakrishna Vasireddi, ^[2] Mohammad Vakili, ^[3] Diana Monteiro, ^[4] Martin Trebbin

^{[1][2][3][4]} University of Hamburg, Centre for Ultrafast Imaging, Luruper Chaussee 149, 22761 Hamburg, Germany

^[1] ramakrishna.vasireddi@uni-hamburg.de ^[2] mohammad.vakili@uni-hamburg.de

^[3] diana.monteiro@uni-hamburg.de ^[4] martin.trebbin@uni-hamburg.de

Abstract—: The synthesis of γ -Fe₂O₃ nanoparticles of varying particle size has been achieved using different molar concentrations of sodium hexametaphosphate while the effect of changing pH has been studied. Iron chloride, sodium hexametaphosphate and sodium hydroxide are used as precursor, reducing agent and accelerator respectively. The synthesized γ -Fe₂O₃ nanoparticles have been characterized by FESEM study, X-ray diffractometry, Raman spectroscopy and UV-vis spectroscopy. The nanoparticle size and morphology are determined by FESEM. From XRD analysis, γ -Fe₂O₃ nanoparticles were found to exhibit tetragonal structure as confirmed from well defined diffraction peaks. The visible photoluminescence (PL) emission from the synthesized γ -Fe₂O₃ nanocrystals has been recorded and peak values are occurred at 370 nm, 371 nm and 373 nm for the pH of 5, 7 and 9 respectively. In case of UV-vis spectra, band gap was estimated and the particle size increased with the increase of the pH values. The synthesized γ -Fe₂O₃ nanoparticles may be extremely useful in biomedical, drug delivery applications

Keywords—: γ -Fe₂O₃ Nanoparticles, Reducing agent, pH, Photoluminescence

I. INTRODUCTION

During recent years, nanoparticles in quantum-size domain have attracted considerable attention in biomedical research field. Nanoparticles, size less than 100 nm retain unique properties due to size effects and surface phenomena at nanoscale. Magnetic nanoparticles (MNPs) are particularly promising an area of increasing interest in the biomedical sciences [1, 2]. For example, targeted drug delivery, magnetic hyperthermia [3, 4], cell labeling with MNPs for in vitro cell separation [5, 6], tissue repair, viable cancer therapy [7, 8] and magnetic resonance imaging (MRI) [9]. However, recent applications of MNPs demonstrate their potential towards decreasing implant infection and increasing tissue growth [10].

Iron oxide nanoparticles are attracted considerable attention in the past decade because of their unique chemical, physical and optical properties leading to numerous potential applications. Furthermore, less sensitive to oxidation so, it could be stable magnetic response. A recent study shows that γ -Fe₂O₃ nanoparticles have promising materials due to their biocompatibility. Currently, there are several protocols for synthesis of iron oxide nanoparticles, for example, pyrolysis [11], co-precipitation [12, 13], gamma-irradiation [14], sol-gel [15] hydrothermal method [16] and chemical methods [17]. The disadvantages of these protocols are that the size uniformity and crystallinity of the iron oxide nanoparticles are rather poor,

and nanoparticle aggregation is commonly observed. However, absolute control over the shape and size distribution of iron oxide nanoparticles remains a challenge, and formation of iron oxide nanoparticles under different conditions still need to be investigated.

In the present work, we report size controlled synthesis of iron oxide nanoparticles by a simple chemical process using sodium hexametaphosphate as reducing agent and sodium hydroxide as an accelerator. The morphological properties were studied by Field Emission Scanning Electron Microscopy (FESEM). Visible photoluminescence emission has been observed from the synthesized iron oxide nanoparticles within the 350-400 nm wavelength range, with peak emissions between 370 and 373 nm.

II. EXPERIMENTAL

Synthesis of iron oxide Nanoparticles

Ferric chloride hexhydrate (FeCl₃·6H₂O), hydrochloric acid (HCl), sodium hexametaphosphate (NaH₂PO₄·2H₂O), Sodium hydroxide (NaOH) and acetone were purchased from analytical grade Merck. Doubly distilled water was used for the process. In a typical procedure, 1 gram of NaOH is added to an aqueous solution of FeCl₃·6H₂O (10 ml, 0.16M) in a flask and then the solution was stirred vigorously at room temperature until pH becomes ~ 11. After the solution centrifuged (6000 rpm for 10 minutes)

and wash the red colour precipitate with distilled water several times till pH becomes ~ 9 . Accordingly, the pH of the red precipitate was adjusted 5, 7 and 9. 100 mL of 0.01M HCl solution was added to the precipitate with Continuous agitation and stirring process was continued for 15 minutes. The above was added to 10 ml of an aqueous solution of $\text{NaH}_2\text{PO}_4 \cdot 2\text{H}_2\text{O}$ (0.08, 0.12 and 0.16M) and added drop wise to above mixture while stirring. Then the colour of solution turned into chocolate brown and it indicates the formation iron oxide (Fe_2O_3) nanoparticles. The obtained chocolate brown transparent sol was heated at about 100°C for 30 min and then cool down to room temperature. The produced reddish brown precipitate was separated by centrifugation (6000 rpm for 10 minutes), subsequently washed with distilled water, and then dried at 100°C in air.

III. CHARACTERIZATION

X-Ray diffraction (XRD) study

The structural characterization of iron oxide nanoparticles were performed using powder X-ray diffraction (PXRD), with the respective nanoparticle powders on glass substrates and the patterns were analysed.

Field emission scanning electron microscopy (FESEM)

For the morphological study of the prepared nanoparticle samples, field emission scanning electron microscopy (FESEM, Carl Zeiss Ultra 55 model) of the centrifuged samples was performed. The average particle size of the prepared iron oxide nanocrystals were determined using Sigma Scan Pro software.

Raman spectroscopy

Room temperature Raman spectroscopy was performed using a LABRAM-HR800 Laser Raman Spectrometer with 514 nm laser radiation. To avoid laser heating of the samples, the incident power was kept at a low value of 1.99 mW.

UV-vis spectroscopy

The optical absorption property of the iron oxide nanoparticles were monitored on a double-beam spectrophotometer (Hitachi, U-3010) with the samples dispersed in distilled water and kept in a quartz cuvette of path length of 10 mm.

Photoluminescence (PL) spectroscopy

The photoluminescence emission spectra from the samples (dispersed in distilled water) were recorded with a Spectrofluorometer (LS 55, Perkin Elmer) at room temperature using a rectangular polished quartz cuvette with a path length of 10 mm.

IV. RESULTS AND DISCUSSIONS

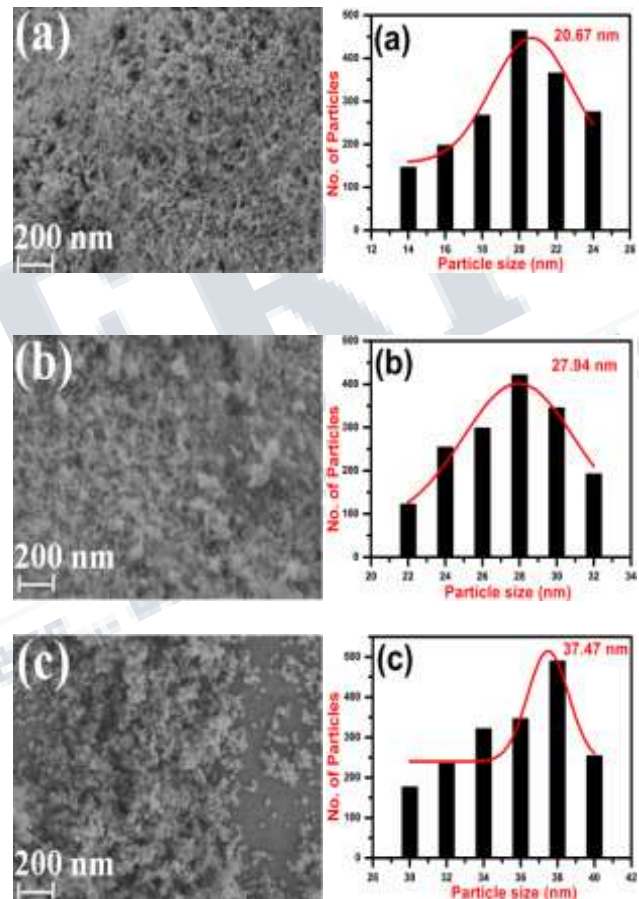


Fig.1: FESEM pictures and size distributions of γ - Fe_2O_3 Nanoparticles.

The surface morphology characteristics of the iron oxide nanoparticles have been studied by field emission scanning electron microscopy. Figure 1 shows the FESEM images of Fe_2O_3 nanoparticles prepared by the chemical method. From the figure it can be observed that the iron oxide nanoparticles have the shape of spherical and the particle size distribution which is varying from 20-40 nm.

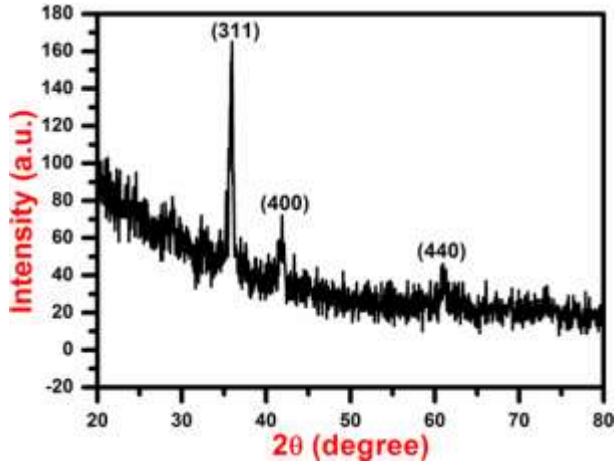


Fig.2: XRD Pattern of γ -Fe₂O₃ nanoparticles

Figure shows an XRD pattern revealing structure characterization of a powder of maghemite nanoparticles obtained by the above chemical method. As shown Diffraction peaks in Fig.2, with characteristic indices (220), (400), and (511), were recognized from the XRD pattern (JCPDS file No.25-1402). The observed diffraction peaks agree well with the tetragonal structure of maghemite. The average lattice parameter calculated below at different 2θ values corresponding to different peaks in the XRD spectra was 8.25 Å for pure γ -Fe₂O₃ nanoparticles. These calculated values of lattice parameter are slightly less than the value of bulk γ -Fe₂O₃ (8.351Å) [18]

Raman Spectroscopy can be used as an effective tool for structural characterization of γ -Fe₂O₃ nanoparticles. The Raman peaks are observed at 1094, 1084 and 1004 cm⁻¹ for different values of pH 9, 7 and 5 respectively. All the Raman spectra presented here consist of narrow peaks and asymmetrically broadened peaks with the different values of full width half-maximum (FWHM) for different pH values. This indicates the low crystal quality of the nanoparticles in tetragonal structure [19]. The Raman peaks shifted to greater wave number with increase of pH values, this is attributed to the greater size of the nanoparticles [20]. From this we would expect that the samples with increasing particle size which could be produced by using different pH concentrations [Fig. 3] to provide good enhancement with a single strong plasmon resonance which is slightly red shifted.

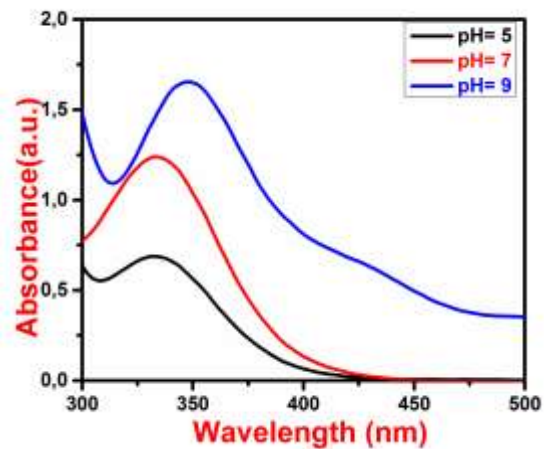


Fig.4: UV-Vis spectra of γ -Fe₂O₃ nanoparticles

Fig.4 shows UV-visible absorption spectrum of Fe₂O₃ nanoparticle at different values of pH. The maximum absorption values are observed at the positions of 332 nm, 335 nm and 348 nm for the different values of pH is 5, 7 and 9 respectively. These absorption peaks were observed in the UV region and near to the lower wavelengths of the visible region. This absorption due to the ligand to-metal charge-transfer transitions and less contribution comes from the Fe³⁺ ligand field transitions of 6A₁ 4T₁(4P) at 332 nm, 6A₁ 4E(4D) & 6A₁ 4T₂ (4D) at 335 nm and 6A₁ 4E; 4A₁(4G) at 348 nm [21].

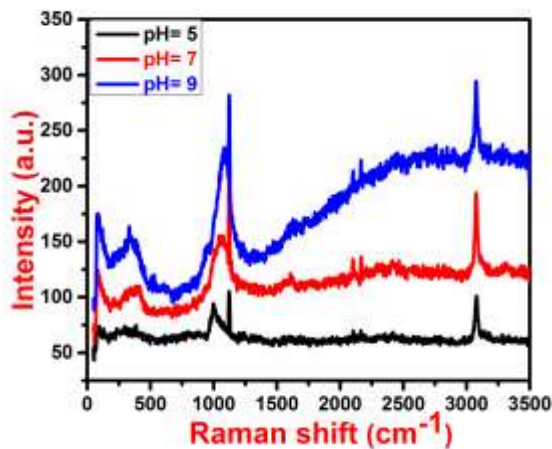


Fig.3: Raman Pattern of γ -Fe₂O₃ Nanoparticles

From this spectrum it can be observed that the absorption peak shifted to longer wavelength with increase of pH values. Therefore, it's known as red shift. This red

shift is presumably due to the formation of larger Fe₂O₃ nanoparticles, which is due to the decrease in charge on the iron oxide particles allowed particle growth by coagulation and aggregation [22]. These results are good agreement with the results obtained using field emission scanning electron microscopy (FESEM) images of iron oxide nanoparticles and their particle size distribution.

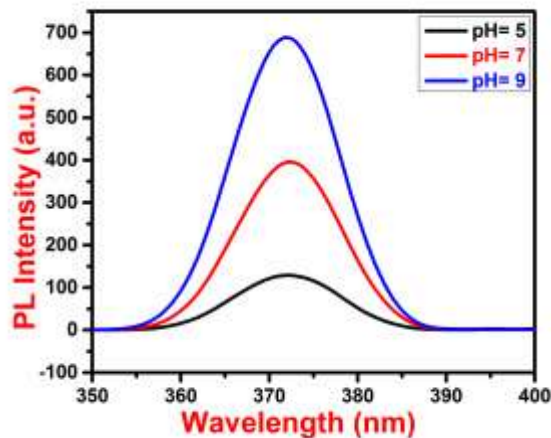


Fig.5: PL spectra of γ -Fe₂O₃ Nanoparticles

The photoluminescence spectra obtained from the synthesized iron oxide nanoparticles are shown in Fig. 5. The PL emission has been obtained within the UV range, from 350 to 400 nm, with the peak positions at 370, 371 and 373 nm for pH 5, 7 and 9 respectively. The PL emission peaks have been found to be red shifted by 38, 36 and 25 nm respectively, from their corresponding UV-vis absorption peaks.

CONCLUSION

We have demonstrated a simple synthesis route to prepare high purity iron oxide nanoparticles with different molar concentrations of sodium hexametaphosphate while the effect of changing pH. The structural characterization of the samples was performed using XRD, Raman spectra and FESEM observations, which led us to infer that the synthesized nanoparticles were tetragonal structure and smaller than 40 nm in size. The UV-visible spectroscopy has shown a shift of the SPR peak, depending upon the changing average particle size of the Ag-NPs, synthesized at different molar concentrations of sodium hexametaphosphate while the effect of changing pH. Visible photoluminescence emission has been observed from the synthesized silver nanoparticles within the 350- 400 nm wavelength range. Such nanoparticles may find wide

applications in biosensor devices, biomedical, drug delivery applications.

ACKNOWLEDGEMENTS

Authors acknowledge the financial support under the University of Hamburg, Centre for Ultrafast Imaging carry out the research.

REFERENCE

- [1] A. Ito, M. Shinkai, H. Honda, T. Kobayashi, "Medical application of functionalized magnetic nanoparticles," *Journal of Biosci Bioeng.* 100(1), 1-11, 2005.
- [2] Q. A. Pankhurst, J. Connolly, S. K. Jones, J. Dobson, "Applications of magnetic nanoparticles in biomedicine," *Journal of Phys D Appl Phys*, 36(13), R167-81, 2003.
- [3] R.S. Molday, L. L. Molday, "Separation of cells labeled with immunospecific iron dextran microspheres using high-gradient magnetic chromatography," *Journal of FEBS Lett*, 170(2), 232-8, 1984.
- [4] J.K. Vasir, V. Labhasetwar, "Targeted drug delivery in cancer therapy," *Journal of Technol Cancer ResT*, 4(4), 363-74, 2005.
- [5] F. Scherer, M. Anton, U. Schillinger, J. Henke, C. Bergemann, A. Kruger, B. Gänsbacher, C. Plank, "Magnetofection: enhancing and targeting gene delivery by magnetic force in vitro and in vivo," *Gene Ther*, 9(2), 102-9, 2002.
- [6] A. Radbruch, B. Mechtold, A. Thiel, S. Miltenyi, E. Pfluger, "Highgradient magnetic cell sorting," *Journal of Method Cell Biol.*, 42, 387-403, 1994.
- [7] A. Jordan, R. Scholz, P. Wust, H. Schirra, T. Schiestel, H. Schmidt, r. Felix, "Endocytosis of dextran and silan-coated magnetite nanoparticles and the effect of intracellular hyperthermia on human mammary carcinoma cells in vitro," *Journal of Magn Mater.*, 194, 185-96, 1999.
- [8] P. Moroz, S.K. Jones, B.N. Gray, "Magnetically mediated hyperthermia: current status and future directions," *Journal of Hyperther.*, 18(4), 267-84, 2002.
- [9] M.F. Kircher, J.R. Allport, M.Zhao, L. Josephson, A.H. Lichtman, R. Weissleder, "Intracellular magnetic labeling with CLIO-Tat for efficient in vivo tracking of

International Journal of Science, Engineering and Management (IJSEM)
Vol 1, Issue 5, September 2016

cytotoxic T cells by MR imaging,” *Journal of Radiology*, 225, 453, 2002.

[10] M. Lewin, N. Carlesso, C. H. Tung, X.W. Tang, D. Cory, D.T. Scadden, R. Weissleder, “Tat peptide-derivatized magnetic nanoparticles allow in vivo tracking and recovery of progenitor cells,” *Journal of Nat Biotechnol.*, 18(4), 410-4, 2000.

[11] N.R. Jana., Y.F. Chen & X.G. Peng, “Size- and shape controlled magnetic (Cr, Mn, Fe, Co, Ni) oxide nanocrystals via a simple and general approach,” *Journal of Chem. Mater.* 16, 3931-3935, 2004.

[12] F.Y. Cheng, C.H. Su, Y.S. Yang, C.S. Yeh, C.Y. Tsai, C.L. Wu, M.T. Wu & D.B. Shieh, “Characterization of aqueous dispersions of Fe₃O₄ nanoparticles and their biomedical applications. *Journal of Biomaterials*,” 26, 729-738, 2005.

[13] R. Vasireddi, R. Paul and A. K. Mitra, “Green Synthesis of AgcoreCushell Nanoparticles: Structural and Optical Characterization,” *Journal of Green Science and Technology*, 1[2], 85-90, (2013).

[14] D.K. Lee, Y.S. Kang, “New synthetic method of magnetite nanocrystallites using c-irradiation,” *Journal of Mol. Cryst. Liq.*, 424, 85-94, 2004.

[15] G.F. Goya, M. Veith, R. Rapalavicuite, H. Shen, S. Mathur, “Thermal hysteresis of spin reorientation at Morin transition in alkoxide derived hematite nanoparticles,” *Journal of Appl. Phys. A-Mater*,” 80, 1523-1526, 2005.

[16] J. Wang, Q. Chen, C. Zeng & B.Y. Hou, “Magnetic-fieldinduced growth of single- crystalline Fe₃O₄ nanowires,” *Journal of Adv. Mater*, 16, 137-140, 2004.

[17] R. Vasireddy, R. Paul and A. K. Mitra, “Green Synthesis of Silver Nanoparticles and the Study of Optical Properties,” *Nanomaterials and Nanotechnology*, 2, 2-8, (2012).

[18] S. Chakrabarti, D. Ganguli, S. Chaudhuri, “Optical properties of γ -Fe₂O₃ nanoparticles dispersed on sol-gel silica spheres”, *Physica E* 24, 333-342, 2004.

[19] R.P. Wang, G.W. Zhou, Y. L. Pan, H.Z. Zhang, D.P. Yu and Z. Zhang, “Gallium assisted plasma enhanced chemical vapor deposition of silicon nanowires”, *Journal of Phys. Rev. B* 61, 6827, 2003.

[20] A. Firat. “New Application For Flotation Of Oxidized Copper Ore”, *Journal of Minerals & Materials Characterization & Engineering*, 4, 2, 67-73, 2005.

[21] D.M. Sherman. The electronic structures of Fe³⁺ coordination sites in iron oxides: Applications to spectra, bonding, and magnetism. *Journal of Physics and Chemistry of Minerals*, 12, 161-175, 2004.

[22] L. Cromieres, V. Moulin, B. Fourest and E. Giffaut, “Physico-chemical characterization of the colloidal hematite/water interface: experimentation and modelling”, *Journal of Colloids and Surfaces A Physicochemical and Engineering Aspects*, 202(1), 101-115, 2002.